Schiff base polymer based on triphenylaminemoieties in themain chain. Characterization and studies in solar cells

C Sanchez, Christian Bernède, Linda Cattin, Mohammed Makha, N Gatica

Thin Solid Films 562 (2014) 495–500

Contents lists available at ScienceDirect

Thin Solid Films

journal homepage: www.elsevier.com/locate/tsf

Schiff base polymer based on triphenylamine moieties in the main chain. Characterization and studies in solar cells

C.O. Sánchez [a], J.C. Bèrnede [b], L. Cattin [c], M. Makha [b], N. Gatica [d]

[a] Instituto de Ciencias Químicas, Facultad de Ciencias, Universidad Austral de Chile, Avda. Las Encinas 220, Campus Isla Teja, Valdivia, Chile
[b] L'UNAM, Moltech Anjou, UMR 6200, 2 rue de la Houssinière, BP 92208, Nantes F-44000, France
[c] L'UNAM, Institut Jean Rouxel (IMN), UMR 6502, 2 rue de la Houssinière, BP 92208, Nantes F-44000, France
[d] Departamento de Polímeros, Facultad de Ciencias, Universidad de Concepción, Avda. Edmundo Larenas 129, Concepción, Chile

ARTICLE INFO

Article history:
Received 5 August 2013
Received in revised form 12 April 2014
Accepted 16 April 2014
Available online 25 April 2014

Keywords:
Synthesis
Polymer
Triphenylamine
Electron donor
Solar cells
Molybdenum oxide
Copper iodide

ABSTRACT

Polytriphenylamine (PTPA), a Schiff base polymer containing triphenylamine (TPA) segments and whose monomer contains triphenylamine and thiophene end groups, was synthesized. The monomer structure enabled the polymerization to be performed under conditions similar to those of thiophene.
Oxidative coupling using $FeCl_3$ as oxidizing agent in anhydrous $CHCl_3$ medium was employed for the polymer synthesis. Scanning electron microscopy, fluorescence spectroscopy, and cyclic voltammetry were used to characterize the polymer. PTPA exhibited high thermal stability with a mass loss of 13.3 % at 546.5 °C. The fluorescence spectrum showed emission at 300–550 nm and the optical band gap was found to be 2.6 eV. It was also established that PTPA forms complexes with Lewis acids, *e.g.* MoO_3 and CuI. Its absorption band widened and extended up to the near-IR. It was seen that PTPA is rich in π-electrons and thus can act as electron donor. The value of the Highest Occupied Molecular Orbital (HOMO) was −5.35 eV indicating its potential application in optoelectronic devices. An attempt was also made to investigate the photovoltaic potential of PTPA. Organic photovoltaic devices with various buffer layer structures, namely ITO/CuI/PTPA/C_{60}/BCP/Al, ITO/MoO_3/PTPA/C_{60}/BCP/Al, and ITO/MoO_3/CuI/PTPA/C_{60}/BCP/Al, where ITO stands for indium tin oxide and BCP for bathocuproine, were utilized for the studies. Power conversion efficiency of these devices ranged between 0.21 and 0.43% under simulated AM 1.5 illumination (100 mW cm^{-2}). This result proved that polymers containing TPA in the main chain hold promising properties that would allow their use in photovoltaic devices.

1. Introduction

Photovoltaic cells made of conjugated polymeric materials hold promise as an alternative source to generate electrical power [1,2]. Synthesis of linear and tri-branched copolymers based on triphenylamine (TPA) as undoped emitting materials and their application in light emitting diodes [3] have been reported. Single-layer electroluminescent devices having the copolymers and polyvinylcarbazole or poly(3,4-ethylenedioxythiophene) as buffer layer, employed as non-doping red-orange emitter as well as electron and hole transport materials, have also been reported. In such single layer devices, preliminary results showed a maximum efficiency of 0.052% [3]. Various other triphenylamine–thienylenevinylene systems as donor materials in heterojunction solar cells were also reported [4]. Besides, star-shaped molecules based on a triphenylamine core with various combinations of thienylenevinylene conjugated branches and electron-withdrawing indanedione or dicyanovinyl groups have been described too. The reported UV-vis absorption and fluorescence emission data of these materials indicated that the introduction of electron-acceptor groups induces an intramolecular charge transfer causing a shift in the absorption onset toward longer wavelengths. Thus, the introduction of electron-acceptor groups in the donor structure induces an extension of the photoresponse in the visible region leading to an increase of the maximum external quantum efficiency and open-circuit voltage under white light illumination. These effects contributed to achieving a conversion efficiency of 1.20% [4]. Other TPA-derivatives of low molecular weight have also revealed diode properties. Higher electrical conductivity and photocurrent observed in these materials were ascribed to TPA units [5].

A series of poly(azomethines) with TPA units in the main chain were found to emit blue light and their photoluminescence to decrease from 30 to 20 % owing to the effect of several organic dopants [6]. Amine groups functionalized TPA was used in the synthesis of these poly(azomethines). 4,4′-Bisamine-triphenylamine condensed with several aromatic dialdehydes exhibited great hole drift mobility indicating they may be utilized as hole transport layer. In addition, they showed remarkable heat resistance [7,8]. Reports about non-polymeric molecules with excellent electron injection properties are also available. This property is attributed to the high electron donor ability of TPA units in the molecules core [9]. Polymers with low band gap (1.65–1.67 eV) and broad absorption band, with extended edge up to 800 nm, were also reported and tested in photovoltaic devices with power conversion efficiency greater than 1.1% [10].

http://dx.doi.org/10.1016/j.tsf.2014.04.071
0040-6090/

In this context the aim of this investigation is to study a Schiff base polymer containing TPA units in the main chain. The monomer contains terminal thiophene moieties that enable its polymerization in conditions similar to those of thiophene. The polymer was characterized by elemental analysis, thermogravimetry, cyclic voltammetry and spectrometry. Furthermore, efforts were made to test the organic semiconductor polymer in photovoltaic devices with different structures containing buffer layers of two Lewis acids, namely MoO_3 and CuI.

2. Experimental

2.1. Measurements

Fourier transform infrared spectroscopy (FT-IR) spectra were recorded on a JASCO FT-IR 4200 spectrometer. Nuclear Magnetic Resonance (NMR) spectra were recorded using tetramethyl silane as internal reference on a 400 MHz Bruker spectrometer. Elemental analyses were conducted on an EA-1108 Fisons Elemental Analyzer. UV–Vis spectra were run on a Perkin-Elmer Lambda 35UV/VIS spectrometer. The spectrum of a 67 mg L^{-1} polytriphenylamine (PTPA) solution was run in dimethyl sulfoxide (DMSO). Optical measurements using the photovoltaic devices were conducted at room temperature using a Carry spectrometer. Fluorescence spectra were recorded on a Jasco FP-6200 spectrofluorometer using a 10 mg L^{-1} PTPA solution in DMSO. Thermogravimetric measurements were carried out on a Thermogravimetric Analyzer Netzsch Iris TG 209 F1. The sample (3 mg) was placed on the balance pan and heated, under nitrogen flow (250 mL min^{-1}), between 30 and 550 °ºC at 20 °C min^{-1} heating rate to obtain the corresponding thermal decomposition profile.

Electro-polymerization was performed using a standard three-electrode cell. The working electrode was a 1.0 × x 0.5 cm^2 indium tin oxide (ITO) coated glass substrate; the counter electrode was a Pt wire, and the reference electrode Ag/AgCl. Unless otherwise stated, all potentials quoted in the current work are referred to this reference electrode. Monomer electropolymerization was accomplished from an anhydrous CH_3CN solution containing 67 mg L^{-1} of monomer and 0.05 M tetrabutylammonium hexafluorophosphate ($TBAPF_6$) as supporting electrolyte. Cyclic voltammograms were recorded at 50 mV s^{-1} scan rate.

2.2. Photovoltaic devices preparation

The 25 mm × 25 mm ITO coated glass substrates used as anode in this study were purchased from SOLEMS. Some ITO needed to be removed to prepare the cell. After coating 20 mm × 25 mm of the 25 mm × 25 mm plate with tape, ITO was removed using Zn powder and diluted HCl. After scrubbing with soap, the whole substrate was rinsed with distilled water, dried and then placed into a vacuum chamber. Several layers were deposited upon the substrate by high-vacuum sublimation at 10^{-4} Pa. The layers were deposited in the following order: MoO_3 and/or CuI, PTPA, fullerene (C_{60}), bathocuproine (BCP) and aluminum. MoO_3 and/or CuI, the anode buffer layer, improves hole collection across the ITO/PTPA interface [11]. PTPA is the electron-donor and C_{60} the electron-acceptor. The BCP layer, called the exciton-blocking layer, improves the electron donor (ED) contact. Aluminum is the cathode. The effective area of each cell was 0.16 cm^2. *In situ* thin-film thickness was estimated using a quartz monitor. Finally, the cell arrangement was: ITO/CuI/PTPA/C_{60}/BCP/Al; ITO/MoO_3/PTPA/C_{60}/BCP/Al; and ITO/MoO_3/CuI/PTPA/C_{60}/BCP/Al. The characteristics of the photovoltaic cells were measured using a calibrated solar simulator (Oriel 300 W) at 100 mW cm^{-2} light intensity adjusted with a reference cell (0.5 cm^2 $CuInGaSe_2$ solar cell, calibrated at NREL, USA). Measurements were conducted under ambient conditions.

Morphology of the different structures used as anode was monitored using scanning electron microscopy (SEM) on a JEOL 7600F scanning electron microscope at the Micro characterization Center of Nantes University.

2.3. Reagents

Aniline, p-fluoro-nitrobenzene, CsF, DMSO, Pd/Carbon 10%, hydrazine monohydrate, and thiophene-2-carboxaldehyde were purchased from Sigma-Aldrich. $FeCl_3$, benzene and p-toluensulfonic acid were from Merck.

4,4′-Bisamine-triphenylamine was prepared in two steps; in the first one the dinitro compound was synthesized while in the second the diamine compound was prepared. The dinitro compound was reduced using hydrazine and 10% Pd/Carbon as catalyst. The obtained 4,4′-bis amino-triphenylamine was condensed with 2 mol of thiophene-2-carboxaldehyde to afford the monomer. The polymer was synthesized by oxidation with $FeCl_3$ according to Fig. 1.

3. Synthesis

3.1. Synthesis of 4,4′-bisdinitro-triphenylamine:

In a 50-mL round-bottom flask, fitted with a reflux condenser, 6.08 g CsF and 28 mL DMSO were placed. The mixture was stirred at room temperature for 30 min and then heated for 10 min under stirring. Subsequently, 1.88 g of aniline and 2.88 g of p-fluoro-nitrobenzene were added. The mixture was then refluxed under stirring for 7 h (checked by TLC, spotted using acetone and eluted with $CHCl_3$/n-hexane (3 + 3 v/v)). The warm mixture was poured into 30 mL methanol, left standing for 1 h, and finally filtered. The yellow solid thus obtained was washed with the filtrate and then with a little of cold methanol. The di-nitro-compound was oven-dried at 40 °C for 2 h. 2.45 g (38% yield) was obtained; mp 196–197 °ºC. Elemental analysis was C 64.37; H 3.85; N 12.75 and O = 19.3% (by difference). The obtained mol/mol ratios were C/N 18/3.05 and C/O 18/3.99. FT-IR (KBr): C–H at 3104 cm^{-1} and 3070 cm^{-1}, C═C at 1599 cm^{-1} and 1499 cm^{-1}, γC–H (para-disubstitution pattern) at 843 cm^{-1}, and γC–H (mono-substitution pattern) at 749 cm^{-1} and 699 cm^{-1}.

3.2. Synthesis of 4,4′-bis amino-triphenylamine

A 250 mL round-bottom flask, equipped with a reflux condenser, was charged with 4.3 g dinitro compound, 140 mL ethanol, and 210 mg 10% Pd/C catalyzer. The mixture was stirred and heated to boiling and 4.2 g hydrazine monohydrate was then slowly added and next refluxed for 215 min (checked by TLC, line spotted using acetone and eluted with ether). The warm mixture was filtered using a Buchner funnel. The filtrate was then concentrated by evaporation until *ca.* 40% of the total volume remains. The mixture was subsequently cooled at

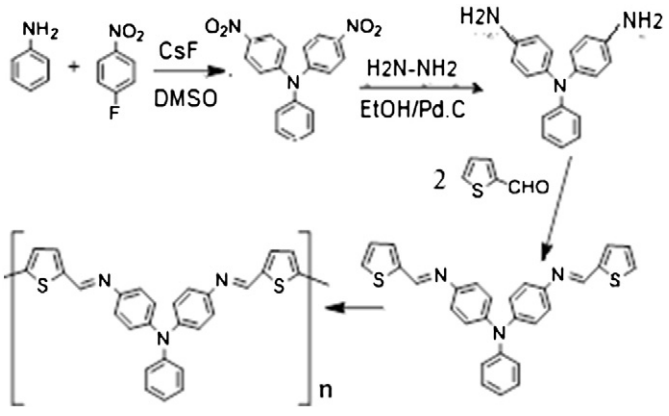

Fig. 1. Monomer and polymer synthesis scheme.

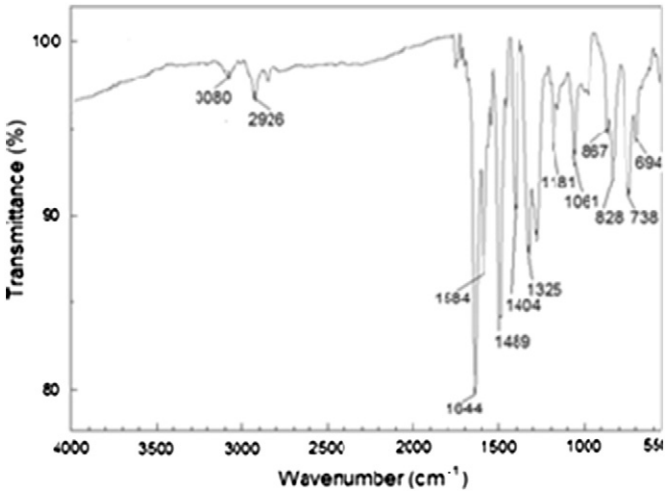

Fig. 2. PTPA FT-IR spectrum.

room temperature (90 min), filtered using a Buchner funnel and the resulting solid washed with mother-liquor and finally with a little volume of cold ethanol. The diamine compound was oven-dried at 50 °C for 2 h. Yield 59% (2.08 g). mp = 177 °C (decomposed). ^{1}H NMR (DMSO-d6): monosubstituted phenyl ring, T (1H, 6.69 ppm), T (2H, 7.08 ppm), d (2H, 6.76 ppm), p-disubstituted two rings; d (4H, 6.65 ppm), d (4H, 6.87 ppm), s (4H, 4.60 ppm). Elemental analysis: C 78.89; H = 6.43; N = 15.41; ratios mol/mol found C/N = 18/3.01 and C/H = 18/18. FT-IR (KBr): νNH2 at 3418, 3339 and 3204 cm^{-1}, νCH at 3050 and 3030 cm^{-1}, νC═C at 1618, 1603 and 1494 cm^{-1}, νCN at 1330 cm^{-1}, γCH (para-disubstitution pattern) at 828 cm^{-1}, and γCH (mono-substitution pattern) at 754 and 694 cm^{-1}.

3.3. Monomer synthesis

A 50 mL round-bottom flask, fitted with a Dean-stark trap and reflux condenser, was charged with 0.60 g of 4,4′- bis amino-triphenylamine, 30 mL benzene and 80 mg p-toluensulfonic acid as catalyst. The mixture was heated and then 0.51 g of 2-thiophenecarboxaldehyde dissolved in 12 mL benzene was added under stirring. The mixture was refluxed for 90 min (checked by TLC, eluted with $CHCl_3$). The hot mixture was filtered and the solvent removed from the filtrate. The residue was dissolved in the minimum possible amount of hot benzene and the resulting black solid was precipitated by adding n-hexane. The supernatant was poured

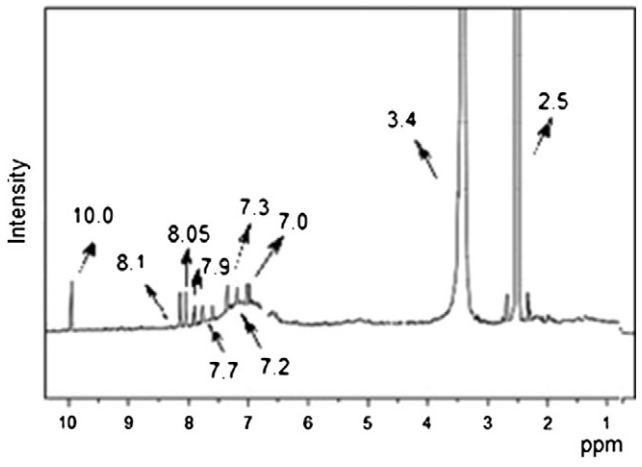

Fig. 3. ^{1}H NMR spectrum PTPA in DMSO-d_6.

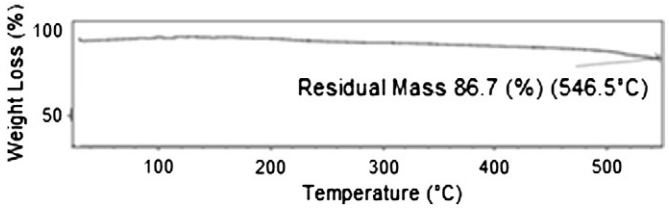

Fig. 4. PTPA thermogram.

into a flask and the solvent wholly removed. The obtained yellow solid was dissolved in the minimum amount of acetone and the monomer precipitated by adding water. The yellow solid was separated by vacuum filtration and finally air-dried. Yield 0.25 g. ^{1}H NMR (DMSO-d_6): m(3H, 7.08 ppm), T(2H, 7.35 ppm), d(4H, 7.05 ppm), d(4H, 7.25 ppm), Imine s (2H, 8.82 ppm), d(2H, 7.65 ppm), T(2H, 7.35 ppm), d(2H, 7.80 ppm). Elemental analysis: C 72.4; H 5.4; N 9.0; S 13.0%. mol/mol ratios C/N 28/2.98; C/H 28/25 and C/S 28/1.9. mp 74-75 °C. FT-IR (KBr): νCH at 3070 and 3025 cm^{-1}, νCH═N at 1614 cm^{-1}, νC═C at 1593 and 1494 cm^{-1}, νCN at 1315 cm^{-1}, γCH (para-disubstitution pattern) at 843 cm^{-1}, γCH (benzene ring mono-substitution pattern) at 754 and 694 cm^{-1}; and γCH (thiophene ring mono-substitution pattern) at 708 cm^{-1}.

3.4. Polymer synthesis

In a 50 mL round-bottom flask, fitted with reflux condenser, 52 mg of monomer and 16 mL of dried $CHCl_3$ were placed. The mixture was boiled and under stirring the warm supernatant (6 mL) was poured into a solution of 0.20 g of anhydrous $FeCl_3$ dissolved in 8 mL of dried $CHCl_3$. This mixture was refluxed for 120 min (checked by TLC, eluted with $CHCl_3$) and then filtered utilizing a Buchner funnel. The final product was a black solid that was thoroughly washed with $CHCl_3$ and then oven-dried at 30 °C. Yield 48 mg.

4. Results and discussion

4.1. Polymer characterization

Monomer and polymer synthesis scheme is shown in Fig. 1. 4,4′-Bisaminotriphenylamine synthesis has been reported [12] and despite one synthesis step was not reproducible, the synthesis was finally achieved using the modified Liou et al. approach [13]. The monomer synthesis was conducted by condensation of the diamine compound with 2 mol of thiophene-2-carboxaldehyde in non-polar medium (benzene). In polar solvents the synthesis is not possible because of components separation and subsequent precipitation of a byproduct. Monomer yield was low because loss occurs by the formation of a difficult-to-break adduct with the catalyst which, in addition, proved to be insoluble in the reaction medium. Monomer characterization by FT-IR and ^{1}H-NMR spectroscopy and elemental analysis agrees well with the thought structure.

Polymer synthesis was complicated because the monomer does not polymerize in the presence of small amounts of water and decomposes, through imine groups, after long stay into the reaction medium. The optimum reaction time was 2 h. Fig. 2 shows the FT-IR spectrum of the polymer and the more significant bands were νCH at 3080 and 2926 cm^{-1}, νCH═N at 1644 cm^{-1}, νC═C at 1584 and 1489 cm^{-1}, νC–N at 1325 cm^{-1}, γCH (para-disubstitution benzene pattern) at 828 cm^{-1}, and γCH (di-substituted thiophene ring) at 738, and 694 cm^{-1} [14,15]. PTPA elemental analysis was C 55.9, H 3.4, N 7.5, and S 9.1 % and the obtained mol/mol ratio C/N 28/3.2; C/H 28/20; and C/S 28/1.7. These results corroborated the proposed structure. However, the percentage of sulfur is slightly low due to cleavage of some

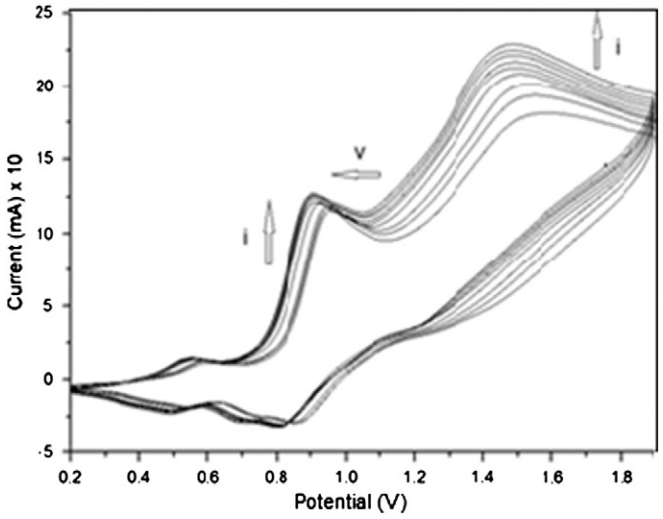

Fig. 5. Electropolymerization (CV) of 67 mg L^{-1} monomer in 0.05 M $TBAPF_6$ supporting electrolyte in dry acetonitrile.

bonds. The presence of the imine group (–CH═N) in the polymer was confirmed by ^1H NMR spectroscopy. Fig. 3 shows the spectrum and the prominent peak associated to the imine group that appears at 10 ppm. Other peaks between 6.5 and 8.3 ppm are associated to aromatic CH. The peak at 2.6 ppm corresponds to the deuterated solvent and the one at 3.5 ppm to water in the solvent.

Prior to vacuum sublimation for polymer thin film deposition, the thermal stability of the polymer was studied by using thermogravimetric analysis. Fig. 4 shows PTPA thermogram. The polymer exhibited a high heat resistance since above 546.5 °C 13.3% weight loss occurred and at 520 °ºC the loss was 10%. Given that during polymer sublimation the temperature was not higher than 250 °C, the deposition process is not expected to induce polymer degradation.

Fig. 5 shows PTPA cyclic voltammograms. Two main redox curves were obtained, with oxidation peaks at 0.95 and 1.45 V.

It is seen that as the number of cycles increases so does the current, evidencing the semiconductor properties of the material. On increasing the number of cycles, both peaks at 0.95 V and 1.45 V shifted toward more cathodic potential, indicating conjugation increase [15].

The onset of monomer oxidation was found to take place at *ca.* 0.75 V and the first oxidation peak potential occurred at 0.95 V. The values are slightly similar to those of thiophene derivatives bonded to electron-donor groups [16,17]. The oxidation peak at 1.45 V that appears as a wide wave in Fig. 5, corresponds to a polymer whose structure contains different conjugation lengths. Different conjugation lengths in poly(thiophene) was reported by Link et al. [15]. Highest Occupied Molecular Orbital (HOMO) can be inferred from the cyclic

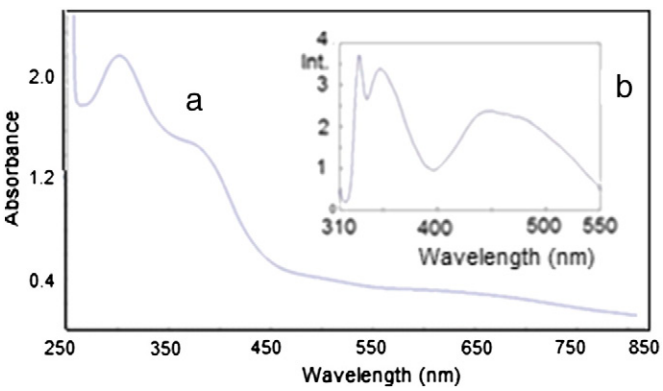

Fig. 6. PTPA spectra in DMSO: a) absorption, b) fluorescence emission.

Table 1
Typical cell parameters.

PTPA thickness (nm)	V_{oc} (V)	J_{sc} (mA cm^{-2})	FF (%)	η	R_s (Ω)	R_{sh} (Ω)
10	0.225	1.04	41.5	0.10	3.3	755
20	0.370	2.56	45	0.43	5.3	760
25	0.430	1.43	36	0.22	22	750

voltammogram [18] according to the equation below and was found to be −5.35 eV.

$$E(HOMO) = ((E_{ox})_{onset} + 4.4)eV = (0.95 + 4.4) = -5.35\ eV.$$

Fig. 6 shows PTPA absorption and emission fluorescence spectra. The absorptions correspond to π–π* and n–π* transitions. The excitation wavelength was 310 nm. Besides, it was observed that PTPA presented a wide emission spectrum between 310 and 550 nm.

For optical band-gap (E_g) measurements an approximation of the Tauc equation [19–24] with data obtained by UV–Vis spectrometry was employed

$$A = B\left(h\nu - E_g\right)^{1/2}/h\nu$$

where A is absorbance, B material constant, h Planck constant and ν frequency. If $A = 0$, $h\nu = E_g$. The optical band-gap is then obtained by plotting $(A\ h\nu)^2$ *vs.* $h\nu$ to give 2.6 eV. Using the HOMO value and this band gap, the corresponding Lowest Unoccupied Molecular Orbital (LUMO) was worked out as −2.75 eV.

4.2. Organic solar cell performance

Firstly, the thickness of the polymeric film was optimized. MoO_3/CuI bilayer was used as anode buffer layer. Typical parameters evaluated for the assembled organic photovoltaic cells devices, namely open circuit voltage V_{oc}, short circuit current J_{sc}, fill factor FF and power conversion efficiency η, are included in Table 1. Besides, series (R_s) and shunt (R_{sh}) resistances are included. $1/R_s$ and $1/R_{sh}$ are defined as the slope at the short circuit point and at the open circuit voltage and are, respectively, the inverse value of R_{sh} and R_s of the equivalent circuit scheme of a solar cell [25].

From Table 1, it can be inferred that the optimum thickness of the polymer layer was 20 nm. For thinner films, light absorption is insufficient and therefore J_{sc} as well as V_{oc} decrease. For thicker films the conductivity of the organic material is low and the R_s value increases significantly provoking a sharp decrease of FF and J_{sc}.

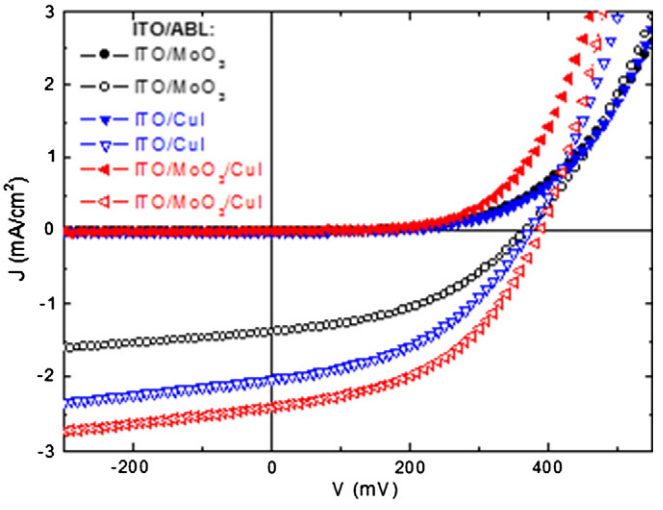

Fig. 7. Typical *J–V* characteristic of glass/ITO/ABL/PTPA/C_{60}/BCP/Al structures, in the dark (full symbol) and under illumination of AM1.5 solar simulation (hollow symbol).

The performance of organic photovoltaic cells using different anode buffer layers (ABL) are presented in Fig. 7. It can be seen that the most varying parameter is J_{sc}. The worst result was obtained with MoO_3 alone as anode buffer layer while the best result was achieved with the MoO_3/CuI bilayer. In order to understand this behavior, ITO/ABL/PTPA multilayer structures were characterized by SEM, optical and electrical measurements.

As shown in Fig. 7, J_{sc} was the parameter that underwent the most significant improvement.

To understand the effect of the different ABL, a specific investigation concerning to surface morphology of the PTPA films after deposition on different ITO ABL anodes was conducted. The surface morphology of the different films is depicted in Fig. 8. It was observed that when sublimated upon the different anode buffer layers, the morphology of the polymeric materials remained almost unchanged.

Another likely improvement is absorbance increase of the organic layer when deposited on a specific ABL. For instance, the absorbance of copper phthalocyanine (CuPc) films is significant when deposited on CuI ABL [26]. From Fig. 9 it seems that a slight absorbance increase of the organic layer takes place when deposited upon MoO_3/CuI. Such increase may contribute to J_{sc} improvement, although the increase is not high enough to justify the J_{sc} change observed in Fig. 7.

Another possible explanation is an enhancement of the organic layer conductivity due to the influence of the CuI anode buffer layer on PTPA properties. To check the conductivity of ED films, hole only structures were prepared. The device was assembled using the same ITO coated glass substrate than that used to fabricate organic photovoltaic cells. After ABL deposition, a 30 nm thick PTPA film was deposited on it. On top of the organic film, a 7 nm thick MoO_3 layer was coated, followed by the aluminum layer. *J–V* characteristics of devices with MoO_3 and CuI buffer layers were investigated and the results are seen in Fig. 10. Charge transport in these devices is limited to holes. Electron injection from the top can be neglected as a result of the large electron barrier caused by the MoO_3 interlayer. The device using CuI ABL exhibits the largest current density at the same driving voltages as compared to a device using MoO_3 ABL. Clearly the conductivity is enhanced when CuI ABL is employed in place of MoO_3 and this may lead to a J_{sc} increase in solar cells.

On the other hand, it has already been demonstrated that MoO_3 enables improving the band matching between anode and organic materials [11]. The sum of these effects justifies the increased efficiency attained by utilizing a double MoO_3/CuI ABL. Such structure allows adding up the dual function of MoO_3 and CuI, since MoO_3 is very efficient in reducing the hole-injection barrier, as compared to bare ITO, while CuI improves the organic film absorption and conductivity.

5. Conclusions

A Schiff base polymer containing triphenylamine segments was synthesized and characterized utilizing various spectroscopic techniques. It was found that PTPA presents high thermal stability with a mass loss 13.3% at 546.5 °C. FT-IR and ^{1}H NMR characterization revealed that the synthesized polymer, as expected, corresponded to PTPA. The HOMO energy level of PTPA was estimated to be -5.35 eV using cyclic

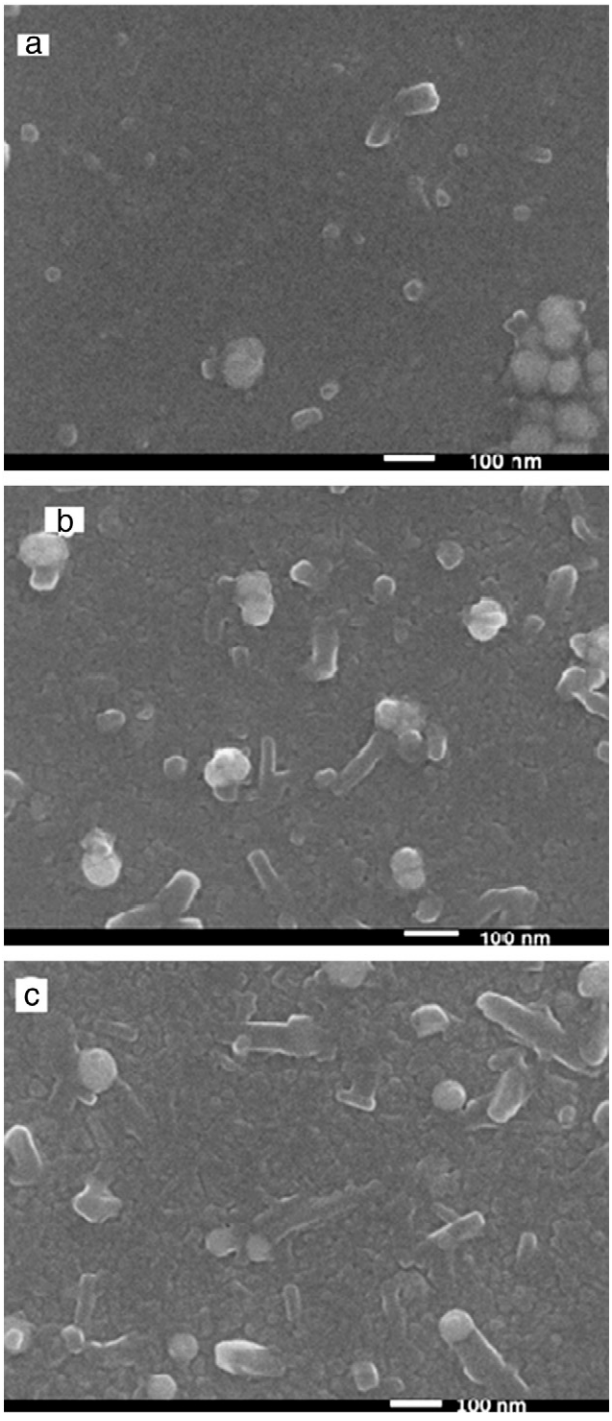

Fig. 8. Micrographs of sublimated material in the presence of a) CuI, b) MoO_3, and c) MoO_3/CuI layers.

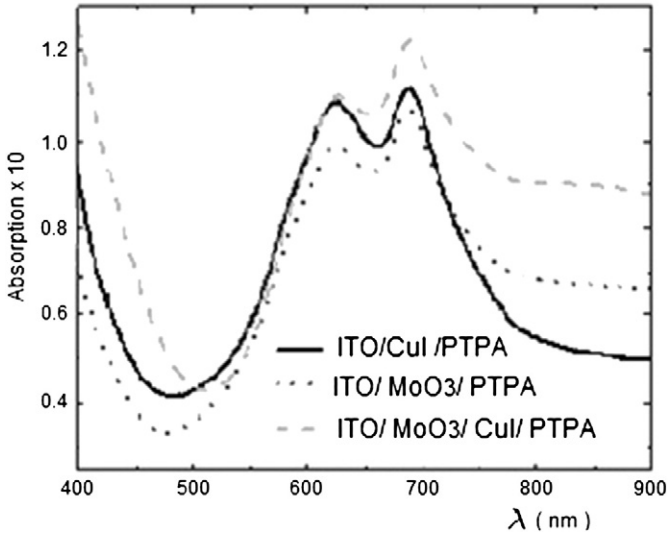

Fig. 9. Absorbance spectra of PTPA thin film deposited onto ITO/CuI (____), ITO/MoO_3 (....) and ITO/MoO_3/CuI (- - -).

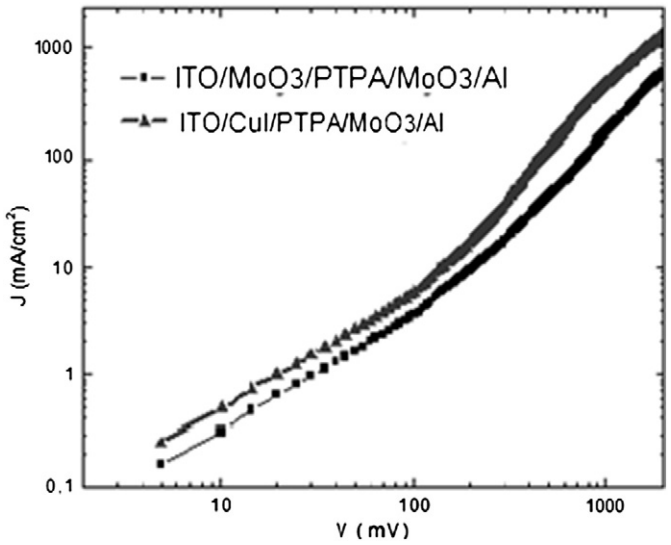

Fig. 10. Typical *J–V* characteristics of glass/ITO/ABL/PTPA/MoO_3/Al structures, with ABL = MoO_3 (■) or CuI (▲).

voltammetry. On the other hand, the measured PTPA band gap using optical studies was 2.6 eV. Utilizing these HOMO and band gap values, the LUMO energy level was worked out as-2.75 eV. These values allow considering the use of PTPA as an electron donor in organic solar cells. Thermal stability studies of the polymer using thermogravimetric analysis demonstrated its high heat resistance, since just 10% of weight loss occurred at 520 °C, while its sublimation temperature is only 250 °C, which warrants PTPA deposition by sublimation without upsetting the polymer.

Consequently, PTPA was employed in planar organic solar cells through vacuum deposition. After optimization of the PTPA thickness it was demonstrated that the highest efficiency is obtained when the ABL is a MoO_3/CuI double layer. Actually, CuI alone increases Jsc by improving the organic film absorption and conductivity, while MoO_3 is highly efficient in reducing the hole-injection barrier. These results proved this double ABL is effective not only with small CuPc molecules but also with polymers such as PTPA.

Acknowledgment

The authors thank Fondecyt financial support through project 1120055.

References

[1] D. Wohrle, D. Meissmer, Organic solar cells, Adv. Mater. 3 (1991) 129.
[2] H. Spanggaard, F.C. Krebs, A brief history of the development to organic and polymeric photovoltaics, Sol. Energy Mater. Sol. Cells 83 (2004) 125.
[3] F. Meng, C. Liu, J. Hua, Y. Cao, K. Chen, H. Tian, Novel linear and tri-branched copolymers based on triphenylamine for non-doping emitting material, Eur. Polym. J. 39 (2003) 1325.
[4] S. Roquet, A. Cravino, P. Leriche, O. Aleveque, P. Frere, J. Roncali, Triphenylamine–thienylenevinylene hybrid systems with internal charge transfer as donor materials for heterojunction solar cells, J. Am. Chem. Soc. 128 (2006) 3459.
[5] K. Sulaiman, M.S. Fakir, Electrical conduction and photovoltaic effects of TPA-derivative solar cells, Thin Solid Films 519 (2011) 5219.
[6] D. Sek, A. Iwan, B. Jarzabek, B. Kaczmarcyk, J. Kasperczk, Z. Mazurak, M. Domanski, K. Karon, M. Lapkowski, Hole transport triphenylamine–azomethine conjugated system: synthesis and optical, photoluminescence, and electrochemical properties, Macromolecules 41 (2008) 6653.
[7] H. Niu, Y. Huang, X. Bai, X. Li, G. Zhang, Study on crystallization, thermal stability and hole transport properties of conjugated polyazomethine materials containing 4,4′-bisamine–triphenylamine, Mater. Chem. Phys. 86 (2004) 33.
[8] H.-J. Niu, Y.-D. Huang, X.-D. Bai, X. Li, Novel poly-Schiff bases containing 4,4′-diamino-triphenylamine as hole transport material for organic electronic device, Mater. Lett. 58 (2004) 2979.
[9] C. Ma, B. Zhang, Z. Liang, P. Xie, X. Wang, B. Zhang, Y. Cao, X. Jiang, Z. Zhang, A novel n-type red luminescent material for organic light-emitting diodes, J. Mater. Chem. 12 (2002) 1671.
[10] J.A. Mikroyannidis, M.M. Stylianakis, P. Suresh, P. Balraju, G.D. Sharma, Low band gap vinylene compounds with triphenylamine and benzothiadiazole segments for use in photovoltaic cells, Org. Electron. 10 (2009) 1320.
[11] L. Cattin, F. Dahou, Y. Lare, M. Morsli, R. Tricot, S. Houari, A. Mokrani, K. Jondo, A. Khelil, K. Napo, J.C. Bernede, MoO_3 surface passivation of the transparent anode in organic solar cells using ultrathin films, J. Appl. Phys. 105 (2009) 034507.
[12] H. Niu, Y. Huang, X. Bai, X. Li, G. Zhang, Study on crystallization, thermal stability and hole transport properties of conjugated poyazomethine materials containing 4,4′-bisamine–triphenylamine, Mater. Chem. Phys. 86 (2004) 33.
[13] G.S. Liou, S.-H. Hsiao, N.-K. Huang, Y.-L. Yang, Synthesis, photophysical, and electrochromic characterization of wholly aromatic polyamide blue-light-emitting materials, Macromolecules 39 (2006) 5337.
[14] S. Tanaka, M.-A. Sato, K. Kaeriyama, Electrochemical polymerization of dithienylethylene, -butadiene and -hexatriene, Makromol. Chem. 186 (1985) 1685.
[15] S. Link, T. Richter, O. Yurchenko, J. Heinze, S. Ludwigs, Electrochemical behavior of electropolymerized and chemically synthesized hyperbranched polythiophenes, J. Phys. Chem. B 114 (2010) 10703.
[16] S.C. Ng, P. Miao, Electrochemical synthesis and characterization studies of poly[3,3′-dialkylsulfanyl-2,2′-bithiophene] films, Macromolecules 32 (1999) 5313.
[17] Y. Wei, C.-C. Chan, J. Tian, G.-W. Jang, K.F. Hsueh, Electrochemical polymerization of thiophenes in the mechanism of the polymerization, Chem. Mater. 3 (1991) 888.
[18] P. Zamora, F.R. Diaz, M. Del Valle, L. Cattin, G. Louarn, J.C. Bernède, Effect of CuI anode buffer layer on the growth of polymers thin films and of the performances of organic solar cells, Nat. Res. 4 (2013) 123.
[19] P. Zamora, F.R. Diaz, M. Del Valle, G. Louarn, L. Cattin, J.C. Bernède, Redox study of polyaniline derivatives for potential use in photovoltaic devices, Int. J. Sci. 2 (2013) 1.
[20] V. Bavastrello, S. Carrara, Optical and electrochemical properties of poly(o-toluidine) multiwalled carbon nanotubes composite Langmuir-Schaefer films, Langmuir 20 (2004) 969.
[21] K. Colladeta, M. Nicolasa, Low-band gap polymers for photovoltaic applications, Thin Solid Films 451–452 (2004) 7.
[22] W. Feng, Z. Qi, Y. Sun, Synthesis and characterization of novel two-component conjugated polythiophenes with 3-octyl and 3-isooctylthiophene side chains, J. Appl. Polym. Sci. 104 (2007) 1169.
[23] B. Sankaran, J. Reynolds, High-contrast electrochromic polymers from alkyl-derivatized poly(3,4-ethylenedioxythiophenes), Macromolecules 30 (1997) 2582.
[24] S. Bhadra, N. Singha, D. Khastgir, Effect of aromatic substitution in aniline on the properties of polyanmiline, Eur. Polym. J. 44 (2008) 1763.
[25] Y. Berredjem, J.C. Bernede, S.O. Djobo, L. Cattin, M. Morsli, A. Boulmokh, On the improvement of the efficiency of organic photovoltaic cells by the presence of an ultra-thin metal layer at the interface organic/ITO, Eur. Phys. J. Appl. Phys. 44 (2008) 223.
[26] L. Cattin, J.C. Bernede, Y. Lare, S. Dabos, N. Seignon, M. Stephant, P. Morsli, P. Zamora, F.R. Diaz, M.A. Del Valle, Improved performance of organic solar cells by growth optimization of CuI/MoO_3 double anode buffer, Phys. Status Solidi A 210 (2013) 802.